

University of Groningen

Quantitative Myocardial Magnetic Resonance Imaging

Triadyaksa, Pandji

DOI:
[10.33612/diss.200241780](https://doi.org/10.33612/diss.200241780)

IMPORTANT NOTE: You are advised to consult the publisher's version (publisher's PDF) if you wish to cite from it. Please check the document version below.

Document Version
Publisher's PDF, also known as Version of record

Publication date:
2022

[Link to publication in University of Groningen/UMCG research database](#)

Citation for published version (APA):
Triadyaksa, P. (2022). *Quantitative Myocardial Magnetic Resonance Imaging*. University of Groningen.
<https://doi.org/10.33612/diss.200241780>

Copyright

Other than for strictly personal use, it is not permitted to download or to forward/distribute the text or part of it without the consent of the author(s) and/or copyright holder(s), unless the work is under an open content license (like Creative Commons).

The publication may also be distributed here under the terms of Article 25fa of the Dutch Copyright Act, indicated by the "Taverne" license. More information can be found on the University of Groningen website: <https://www.rug.nl/library/open-access/self-archiving-pure/taverne-amendment>.

Take-down policy

If you believe that this document breaches copyright please contact us providing details, and we will remove access to the work immediately and investigate your claim.

Downloaded from the University of Groningen/UMCG research database (Pure): <http://www.rug.nl/research/portal>. For technical reasons the number of authors shown on this cover page is limited to 10 maximum.

Chapter 5



Early detection of heart function abnormality by native T1: A comparison of two T1 quantification methods

Pandji Triadyaksa

Dirkjan Kuijpers

Tugba A. D'Antonoli

Jelle Overbosch

Mieneke Rook

J. Martijn van Swieten

Matthijs Oudkerk

Paul E. Sijens

Abstract

Objective

To compare the robustness of native T1 mapping using mean and median pixel-wise quantification methods.

Methods

Fifty-seven consecutive patients without overt signs of heart failure were examined in clinical routine for suspicion of cardiomyopathy. MRI included the acquisition of native T1 maps by a motion-corrected modified Look-Locker inversion recovery sequence at 1.5 T. Heart function status according to four established volumetric left ventricular (LV) cardio MRI parameter thresholds was used for retrospective separation into subgroups of normal ($n = 26$) or abnormal heart function ($n = 31$). Statistical normality of pixel-wise T1 was tested on each myocardial segment, and mean, and median segmental T1 values were assessed.

Results

Segments with normally distributed pixel-wise T1 (57/58%) showed no difference between mean and median quantification in either patient group, while differences were highly significant ($P < 0.001$) for the respective 43/42% non-normally distributed segments. Heart function differentiation between two patient groups was significant in 14 myocardial segments ($P < 0.001$ – 0.040) by median quantification compared with six ($P < 0.001$ – 0.042) by using the mean. The differences by median quantification were observed between the native T1 values of the three coronary artery territories of normal heart function patients ($P = 0.023$) and insignificantly in the abnormal patients ($P = 0.053$).

Conclusion

Median quantification increases the robustness of myocardial native T1 definition, regardless of the statistical normality of the data. Compared with the currently prevailing method of mean quantification, differentiation between LV segments and coronary artery territories is better and allows for earlier detection of heart function impairment.

Keywords

Magnetic Resonance Imaging, Myocardium, Cardiomyopathies, Statistical Distribution

Introduction

Pre-contrast T1 relaxation time, the parameter at stake in native T1 mapping, has shown its potential for identifying myocardial tissue abnormality [1], with the limitation that the values measured are sequence-specific [2–7]. Native T1 increases may indicate disease and have been associated with diffuse myocardial fibrosis in different types of cardiomyopathy [7–15]. Moreover, in patient groups with myocardial impairment, an increase of native T1 was observed in the absence of late gadolinium enhancement (LGE) [7, 9, 10, 14, 15], suggesting that native T1 mapping can be an early indicator of myocardial tissue abnormality. Therefore, a robust native T1 quantification method is needed to ensure early identification of heart function abnormality.

In measuring cardiac T1 value, numerous studies showed normal native T1 variation on different myocardial regions [4, 5, 8, 10, 11, 13, 16–19]. Intersegmental variations complicate the standardization of normal values and disease identification. Pixel-wise T1 value quantification also faces variability due to protocol parameters, sequence design, scanner adjustment, T1 fit model, tissue characteristics, and patient's condition [6, 20]. In view of the heterogeneity of pixel-wise T1 values as illustrated in Figure 5.1, variability may be reduced by the assessment of median values of pixel-wise T1 per segment rather than the evaluation of the means [14].

In liver and heart iron deposition assessment by T2* mapping, pixel-wise median quantification produced lower observer variability compared with mean quantification [21] and lower T2* variability in different myocardial regions [22, 23]. These studies showed that partial volume effect, heart motion artifact, the fitting model used, and observer's myocardial contour determination influence the pixel-wise assessment and quantification in the region of interest. However, pixel-wise native T1 assessment studies published to date used mean quantification with a few ones checking the normality of the statistical distribution of datasets as a whole [11, 13–15, 24] rather than performing statistical normality testing of pixel-wise T1 distribution per segment. This study aims to investigate the normality of pixel-wise T1 values per left ventricular heart segment and subsequently compare the mean and median values. Application of both methods on patients with normal and abnormal heart function is used to assess their potential for early detection of heart function abnormality.

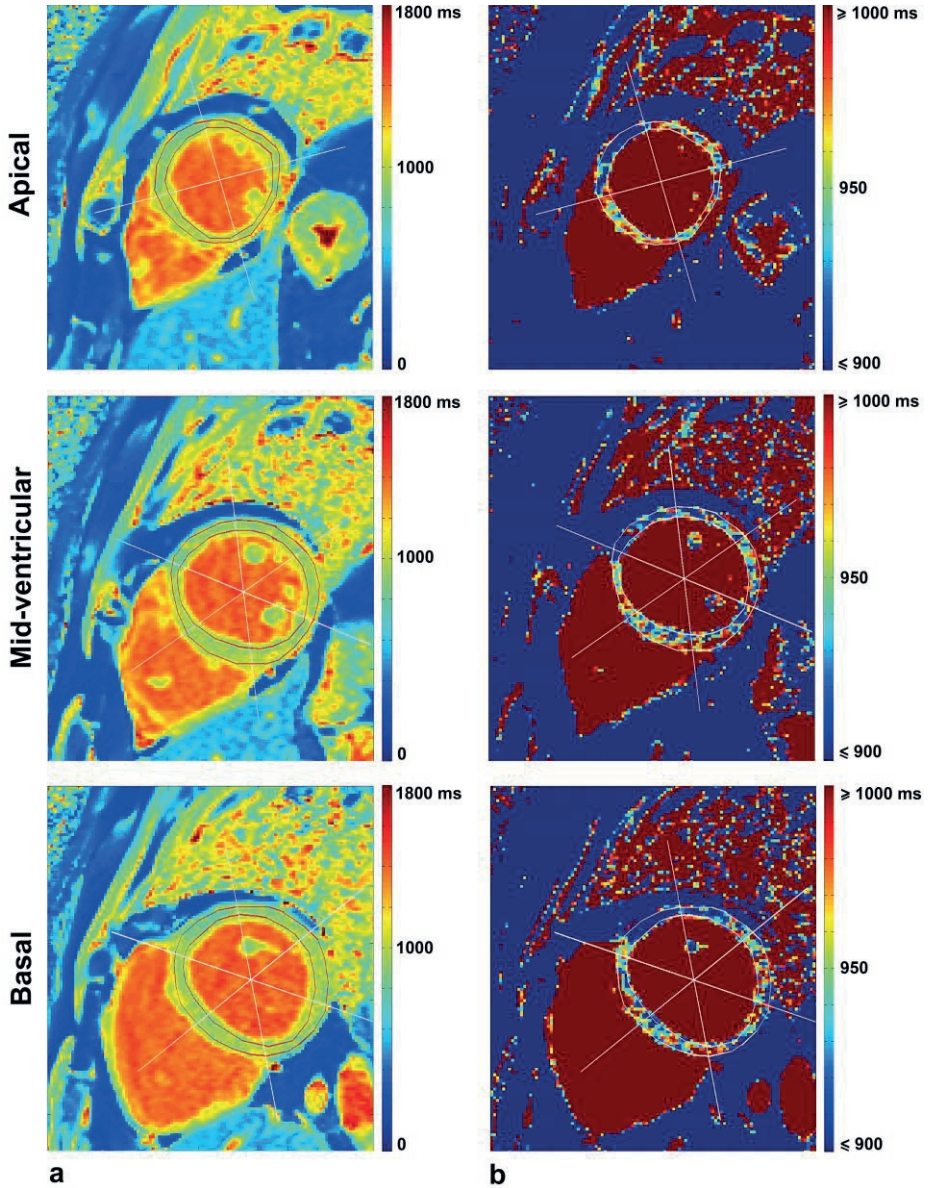


Figure 5.1 Native T1 mapping of the left ventricular myocardium, three short-axis slices segmented by the AHA model in a case of normal heart function scaled (a) from 0 – 1800 ms and (b) from 900 – 1000 ms to show T1 heterogeneity.

Materials and methods

This retrospective analysis was conducted on magnetic resonance imaging (MRI) data acquired from May until October 2015 with approval by the hospital review board waiving the requirement of informed consent. MRI including (native) T1 mapping sequences were used to evaluate 145 consecutive patients examined in clinical routine for suspicion of cardiomyopathy. Patients with overt signs of heart failure, i.e., LGE pattern (observed 10–15 min after 0.2 mmol/kg of gadoterate meglumine: Dotarem, Guerbet), irregular heartbeat, or myocardial wall, and cavum thickening, were excluded. The remaining 57 patients were divided into two groups with either normal or abnormal functional heart magnetic resonance (MR) parameters. Normal heart function was defined as three of four MR parameters (i.e., left ventricle (LV) end-diastolic volume, LV end-systolic volume, stroke volume, and ejection fraction) being within the normal MR parameter ranges and the fourth still within the borderline of normality as defined by Kawel-Boehm et al. [25].

Cardiac magnetic resonance imaging

All MR scans were performed on a 1.5 T whole-body scanner (Aera, Siemens Medical Solutions). Functional heart MR parameters were acquired by performing cine imaging steady-state free precession images with echo time (TE) 1.1 ms, repetition time (TR) 42.1 ms, flip angle (FA) 56°, reconstructed voxel size 1.82 × 1.82 × 8 mm, a field of view (FOV) 349 × 349, matrix 192 × 192, pixel bandwidth 930 Hz, phase resolution sampling 70%, phase FOV 100%, and GeneRalized Autocalibrating Partial Parallel Acquisition (GRAPPA) acceleration factor 2.

Modified Look-Locker inversion recovery (MOLLI) was implemented in a single breath-hold at late diastole, using vendor-provided motion correction for T1 mapping based on image registration with synthetic image estimation [26]. The 5(3)3 MOLLI protocol acquired 5 images after the first inversion pulse, followed by a pause of 3 heartbeats prior to the acquisition of the next 3 images after the second inversion pulse. The protocol's initial inversion time (TI) was 100 ms, TE 1.12 ms, TR 280.56 ms, and FA 35°. Reconstructed voxel size was 1.41 × 1.41 × 8 mm, FOV 306 × 360, matrix 218 × 256, phase resolution sampling 66%, phase FOV 85%, and GRAPPA acceleration factor 2.

Table 5.1 Characteristics of patients with normal and abnormal heart function according to the criteria of Kawel-Boehm et al. [25].

	Normal heart function (<i>n</i> = 26)	Abnormal heart function (<i>n</i> = 31)	<i>P</i> -Value ^a
General parameter			
Number of males	13 (50) ^b	17 (55) ^b	0.716 ^c
Age (years)	47 ± 19	41 ± 18	0.279 ^d
Heart rate (bpm)	67 ± 8	66 ± 7	0.706
BMI (kg/m ²)	25.15 ± 2.50	24.00 ± 2.60	0.481
BSA (m ²)	1.96 ± 0.22	1.97 ± 0.25	0.940 ^d
MR measured parameter			
LV mass (g)	86.67 ± 20.47	105.04 ± 22.14	0.031
LV mass index (g/m ²)	44.11 ± 10.42	53.34 ± 11.24	0.033
LV EDV (ml)	155.97 ± 20.52	214.44 ± 25.91	< 0.001
LV EDV index (ml/m ²)	79.39 ± 10.44	108.89 ± 13.16	< 0.001
LV ESV (ml)	61.23 ± 11.46	101.93 ± 22.48	< 0.001
LV ESV index (ml/m ²)	31.16 ± 5.83	51.76 ± 11.41	< 0.001
Stroke volume (ml)	96.76 ± 11.58	104.55 ± 16.23	0.305
LV EF (%)	61.50 ± 3.87	49.50 ± 6.15	< 0.001 ^d
Cardiac output (L/min)	6.14 ± 1.13	6.50 ± 1.21	0.773

Values are presented as mean ± standard deviation or median ± median absolute deviation or *n* (%). *n* number of patients, *bpm* beats per minute, *BMI* body mass index, *BSA* body surface area, *MR* magnetic resonance, *LV* left ventricle, *EDV* end-diastolic volume, *ESV* end-systolic volume, *EF* ejection fraction.

^a *P*-Values calculated by Mann-Whitney U test.

^b Value is the number of patients, with a percentage in parentheses.

^c *P*-Value by chi-square test.

^d *P*-Values by independent *t*-test.

Image analysis

T1 maps were generated by custom-written software (developed in MATLAB version 7.14, The Math-works) at three short-axis locations (apical, mid-ventricular, and basal) using pixel-wise fitting of a three-parameter model [20]:

$$SI = A - Be^{-TI/T1^*} \quad (5.1)$$

to acquire T_1 as:

$$T1 = T1^*(B/A - 1) \quad (5.2)$$

Where *SI*, *TI* are signal intensity, inversion time, respectively, while *A*, *B* are constant values. Two cardiac radiologists (with 5 and 7 years of experience, respectively) and two non-cardiac experts (a radiology technician with 15 years of experience and a non-cardiac radiologist with less than 1 year experience in

cardiac imaging) manually drew LV endocardial and epicardial contours once on the T1 map while carefully avoiding LV blood pool and epicardial fat (Figure 5.1). Segmental T1 analysis was conducted on all pixels (without applying endocardial/epicardial inset correction) according to American Heart Association (AHA) 16-segment model [19] on global myocardium by averaging the 16 segments, different slice locations, and different coronary artery territories [27]. The volumetric cardiac MR parameters were evaluated by a cardiac imaging post-processing radiology technician using QMASS software (Medis Medical Imaging Systems) and checked by a cardiac radiologist (Table 5.1).

Statistical analysis

Statistical normality testing of data distribution was assessed using the Shapiro-Wilk test using custom-written software (developed in MATLAB version 7.14) [28]. The cardiac MR parameter of a dichotomous variable was compared using the chi-square test, and continuous variables were compared using independent *t*-test or Mann-Whitney U test as appropriate. On normal and abnormal heart function patient groups, each segment T1 quantification was reported both using mean \pm standard deviation (SD) and median \pm median absolute deviation (MAD) [29, 30] regardless of the segment's statistical normality status. On segments having normally distributed and non-normally distributed pixel-wise T1, a comparison between mean and median T1 quantification was assessed by the Mann-Whitney U test. The agreements between mean and median segmental T1 quantification were assessed using the Bland-Altman plot with a limit of agreement (LoA) set to be $1.96 \times$ SD of the difference.

A coefficient of variance (CoV) of the T1 relaxation time was calculated as the SD of the difference divided by the mean and expressed in percentage. Comparison of T1 values between two patient groups on different LV regions was conducted using an Independent sample *t*-test for data evaluated by the mean and the Mann-Whitney U test for data evaluated by the median. Multiple comparisons across myocardial regions were conducted by the Kruskal-Wallis test with the Dunn-Bonferroni post hoc test adjustment. Statistical analyses were performed using IBM SPSS statistics software version 23 (IBM Corporation) with $P < 0.05$ considered statistically significant.

Results

Patient classification

According to the criteria of Kawel-Boehm et al. [25], 26 of 57 patients were classified in the normal heart function group, and the remaining 31 patients were classified in abnormal heart function group with similar general characteristics, such as age, heart rate, body surface area and body mass index ($P > 0.05$). Their characteristics are listed in Table 5.1 (and differentiated by gender, in Supplementary Table S1).

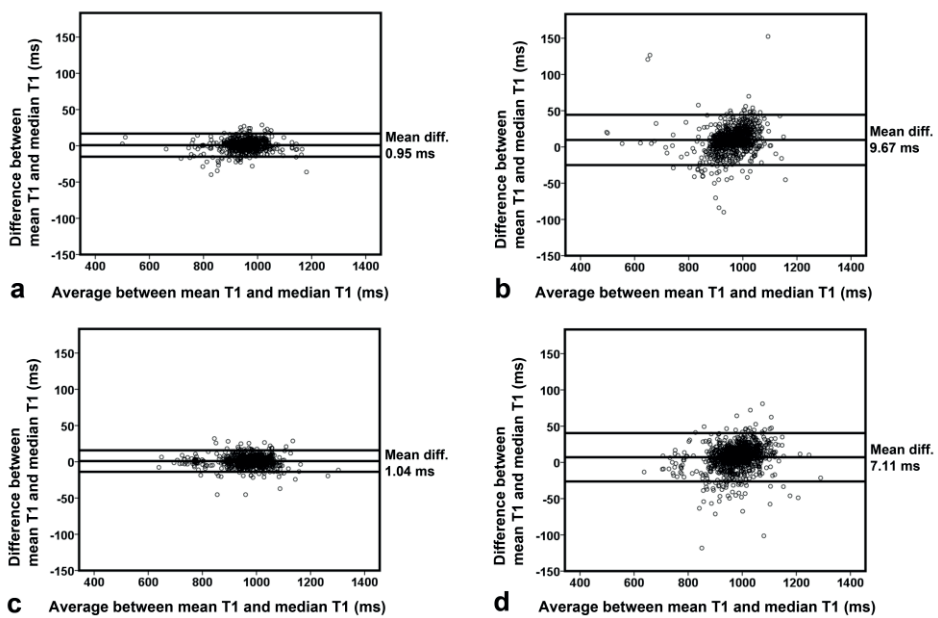


Figure 5.2 Bland-Altman plot assessment of pixel-wise native T1 agreement per segment quantified by means and medians. Quantification, in normal heart function patients, for segments having statistical normally distributed (a) and statistical non-normally distributed pixel-wise T1 (b). Quantification, in abnormal heart function patients, for segments having statistical normally distributed (c) and statistical non-normally distributed pixel-wise T1 (d).

Table 5.2 T1 coefficient of variance between all observers in different left ventricular myocardial regions.

	ns ^a	Patients with normal heart function		ns ^a	Patients with abnormal heart function	
		CoV between observers using			CoV between observers using	
		Mean T1	Median T1		Mean T1	Median T1
Global LV myocardium	2496	5.29	4.88	2976	4.31	3.62
LAD	936	5.33	4.73	1116	4.52	3.59
RCA	780	4.18	3.64	930	3.85	3.12
LCx	780	6.17	6.04	930	4.42	4.05
Basal	936	3.60	2.88	1116	3.29	2.56
1 Anterior	156	4.25	2.73	186	4.71	3.54
2 Anteroseptal	156	2.82	2.40	186	2.32	1.80
3 Inferoseptal	156	2.83	2.50	186	2.45	2.01
4 Inferior	156	2.68	1.78	186	3.34	2.71
5 Inferolateral	156	2.95	2.07	186	2.85	2.21
6 Anterolateral	156	5.12	4.65	186	3.39	2.58
Mid-ventricular	936	5.12	4.52	1116	4.08	3.28
7 Anterior	156	6.37	6.02	186	5.96	4.70
8 Anteroseptal	156	4.04	3.15	186	3.30	2.43
9 Inferoseptal	156	1.91	1.43	186	2.50	1.78
10 Inferior	156	3.44	2.19	186	3.27	2.91
11 Inferolateral	156	5.62	5.00	186	3.39	2.73
12 Anterolateral	156	7.27	6.83	186	4.85	4.09
Apical	624	7.40	7.32	744	5.75	5.14
13 Anterior	156	8.86	8.52	186	6.35	5.33
14 Septal	156	3.34	2.48	186	2.77	2.26
15 Inferior	156	7.83	7.33	186	6.39	5.09
16 Lateral	156	8.53	9.16	186	6.57	6.78

Data are in percentage. *LV* left ventricle, *LAD* left anterior descending, *RCA* right coronary artery, *LCx* left circumflex artery, *ns* number of segments, *CoV* coefficient of variance.

^a The number of segments reflects six combinations of segment comparisons between four observers.

Statistical normality of native T1 data distribution

The assessment of AHA 16 segments of LV myocardium from 26 normal patients and 31 abnormal heart function patients resulted in a total of 416 and 496 segments, respectively. With four observers assessing these segments, we obtained 1664 and 1984 segments, respectively.

In all segments of normal patients, statistical normality testing of pixel-wise native T1 per segment showed that 964 of 1664 segments (58%) were statistically non-normally distributed, whereas, in all segments of abnormal patients, this statistical distribution was found in 1140 of 1984 segments (57%). In segments having statistically normally distributed pixel-wise T1 (subject for mean quantification), segmental T1 quantification by either mean or median showed no significant difference of T1 value in normal heart function group ($P = 0.532$) and abnormal heart function group ($P = 0.628$). This indicates that in statistically normally distributed data, median quantification is equivalent to the use of the mean. For segments with non-normally distributed pixel-wise T1 (subject for median quantification), a significant difference was found between the two T1 quantifications in both normal ($P < 0.001$) and abnormal heart ($P = 0.003$) functional groups. This finding indicates that mean quantification cannot be used for statistical non-normally distributed data.

The Bland-Altman plot confirms these claims in normal heart function patients by showing smaller differences of pixel-wise T1 assessed by mean and median quantification for segments having statistically normally distributed pixel-wise T1 (mean difference of 0.95 ms, CoV of 0.85 %, and LoA of 15.96 ms) (Figure 5.2a) compared to segments with non-normally distributed T1 (mean difference of 9.67 ms, CoV of 1.84 % and LoA of 34.72 ms) (Figure 5.2b). Likewise, in abnormal heart function patients (Figure 5.2c), pixel-wise T1 had a similar smaller Bland-Altman mean difference of 1.04 ms, CoV of 0.78 %, and LoA of 14.83 ms in statistically normally distributed data as opposed to higher Bland-Altman of (mean differences of 7.11 ms, CoV 1.74 % of and LoA 33.39 ms) in non-normally distributed data (Figure 5.2d).

Table 5.3 Mean T1 value in different left ventricular myocardial regions.

	T1 value of patients with normal heart function		T1 value of patients with abnormal heart function		P-Value ^b
	ns ^a	Mean ± SD (ms)	ns ^a	Mean ± SD (ms)	
Global LV myocardium	2496	960.69 ± 60.92	2976	976.75 ± 68.65	< 0.001
LAD	936	958.85 ± 60.73	1116	974.73 ± 71.09	< 0.001
RCA	780	973.35 ± 60.23	930	989.35 ± 64.49	< 0.001
LCx	780	950.24 ± 59.65	930	966.57 ± 67.84	< 0.001
Basal	936	975.23 ± 45.31	1116	982.36 ± 63.21	0.003
1 Anterior	156	961.18 ± 46.10	186	971.17 ± 65.11	0.099
2 Anteroseptal	156	993.88 ± 48.61	186	992.96 ± 62.64	0.879
3 Inferoseptal	156	987.97 ± 42.21	186	993.07 ± 58.92	0.353
4 Inferior	156	987.97 ± 38.09	186	996.81 ± 64.46	0.117
5 Inferolateral	156	969.59 ± 39.13	186	979.66 ± 62.96	0.072
6 Anterolateral	156	950.78 ± 40.28	186	960.47 ± 57.23	0.068
Mid-ventricular	936	961.51 ± 52.86	1116	973.36 ± 64.77	< 0.001
7 Anterior	156	940.11 ± 56.45	186	953.18 ± 70.86	0.064
8 Anteroseptal	156	973.67 ± 45.14	186	977.09 ± 60.32	0.550
9 Inferoseptal	156	980.54 ± 46.28	186	990.38 ± 57.79	0.081
10 Inferior	156	976.31 ± 50.81	186	986.47 ± 58.59	0.091
11 Inferolateral	156	961.45 ± 42.94	186	982.18 ± 62.04	< 0.001
12 Anterolateral	156	936.95 ± 57.11	186	950.85 ± 67.31	0.042
Apical	624	937.66 ± 82.09	744	973.43 ± 80.65	< 0.001
13 Anterior	156	914.57 ± 79.12	186	962.01 ± 80.23	< 0.001
14 Septal	156	969.67 ± 48.66	186	991.98 ± 76.94	0.001
15 Inferior	156	933.98 ± 90.70	186	980.04 ± 79.49	0.004
16 Lateral	156	932.43 ± 92.86	186	959.71 ± 82.10	< 0.01

SD standard deviation, ns number of segment, LV left ventricle, LAD left anterior descending, RCA right coronary artery, LCx left circumflex artery.

^a The number of segments reflects six combinations of segment comparisons between four observers.

^b P-Values of comparison between normal and abnormal heart function groups by independent sample t-test.

Regional T1 analysis and heart function abnormality

In a regional myocardial analysis (Table 5.2), improvement of interobserver reproducibility of segmental T1 values was found for most regional myocardium areas in normal and abnormal heart function patients when using median compared with the mean for its pixel-wise quantification. This was indicated by CoV reductions, whereas results were similar for observers with different cardiac imaging expertise backgrounds (Supplementary Table S2).

Regional T1 analysis of four observers on different LV myocardial regions by using mean and median T1 quantification is presented in Table 5.3 and Table 5.4, respectively. For each table, the statistical normality testing of its data distribution per LV myocardial region is presented by Supplementary Table S3 for native T1 quantified by its mean and by Supplementary Table S4 for native T1 quantified by its median. Tables S3 and S4 show that most of the T1 data from different myocardial regions are statistically non-normally distributed, reflecting inadequate mean quantification in Table 5.3 to differentiate two different patient groups. As a result, the differentiation of T1 values between normal and abnormal heart function groups is undetected in ten of 16 AHA segments of Table 5.3 ($P = 0.059 - 0.879$). When comparing the two patient groups using median quantification (Table 5.4), a significant increase of T1 values is identified in abnormal heart function patients compared to normal heart function in all myocardial regions ($P < 0.001 - 0.024$) with the exception in the mid-ventricular anteroseptal ($P = 0.110$) and basal anterior segments ($P = 0.080$). Heart function differentiation between the two groups is thus concluded to be significant in 14 myocardial segments ($P < 0.001 - 0.040$) by median quantification compared with only six ($P < 0.001 - 0.042$) when using the mean.

Using median quantification, the regional LV T1 value in the normal heart function patient group was found to be significantly different in the three short-axis slices and the three coronary artery territories attributed to the 16 AHA segments (Figure 5.3a) ($P < 0.001 - P = 0.023$). However, in the abnormal heart function patient group (Figure 5.3b), the T1 value between apical vs. mid-ventricular short-axis slices and between left anterior descending (LAD) and left circumflex artery (LCx) coronary artery territories were not significantly different ($P > 0.999$ and $P = 0.053$, respectively).

Table 5.4 Median T1 value in different left ventricular myocardial regions.

	T1 value of patients with normal heart function		T1 value of patients with abnormal heart function		P-Value ^b
	ns ^a	Median ± MAD (ms)	ns ^a	Median ± MAD (ms)	
Global LV myocardium	2496	959.85 ± 30.32	2976	974.94 ± 35.07	< 0.001
LAD	936	958.52 ± 33.29	1116	971.53 ± 35.36	< 0.001
RCA	780	971.78 ± 27.95	930	987.15 ± 37.05	< 0.001
LCx	780	952.39 ± 26.26	930	964.94 ± 33.10	< 0.001
Basal	936	966.94 ± 22.61	1116	980.79 ± 33.98	< 0.001
1 Anterior	156	964.35 ± 24.48	186	969.98 ± 33.09	0.080
2 Anteroseptal	156	976.65 ± 20.45	186	1004.20 ± 39.28	0.040
3 Inferoseptal	156	971.14 ± 19.05	186	987.85 ± 36.06	< 0.001
4 Inferior	156	981.81 ± 25.15	186	990.10 ± 39.13	0.010
5 Inferolateral	156	964.20 ± 24.18	186	981.66 ± 30.88	< 0.001
6 Anterolateral	156	957.23 ± 16.38	186	960.54 ± 28.07	< 0.001
Mid-ventricular	936	956.61 ± 31.27	1116	972.02 ± 33.83	< 0.001
7 Anterior	156	938.52 ± 39.88	186	953.70 ± 28.24	< 0.001
8 Anteroseptal	156	965.38 ± 30.20	186	972.83 ± 34.06	0.110
9 Inferoseptal	156	970.71 ± 22.85	186	982.84 ± 32.18	< 0.001
10 Inferior	156	972.89 ± 27.91	186	996.98 ± 32.71	< 0.001
11 Inferolateral	156	951.55 ± 22.85	186	981.01 ± 30.19	< 0.001
12 Anterolateral	156	932.91 ± 31.00	186	946.04 ± 33.09	0.010
Apical	624	940.58 ± 39.64	744	971.31 ± 37.26	< 0.001
13 Anterior	156	919.70 ± 41.48	186	962.45 ± 31.95	< 0.001
14 Septal	156	959.46 ± 36.14	186	980.53 ± 37.96	< 0.001
15 Inferior	156	936.24 ± 46.59	186	982.10 ± 43.85	< 0.001
16 Lateral	156	953.10 ± 36.88	186	965.16 ± 49.61	< 0.001

MAD median absolute deviation, ns number of segments, LV left ventricle, LAD left anterior descending, RCA right coronary artery, LCx left circumflex artery.

^a The number of segments reflects six combinations of segment comparisons between four observers.

^b P-Values of comparison between normal and abnormal heart function groups by Mann-Whitney U test.

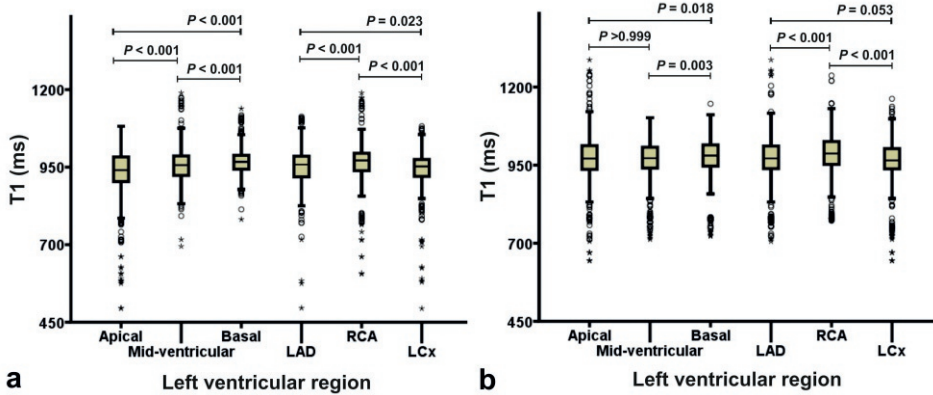


Figure 5.3 Boxplot of median T1 in different left ventricular myocardial regions. Quantifications for normal (a) and abnormal (b) heart function patients. Comparisons between the regions were conducted by the Dunn-Bonferroni post hoc test adjustment of the Kruskal-Wallis test result.

Discussion

This study shows that median value quantification can be used for segmental native T1 assessment regardless of the distribution of pixel values and, therefore can replace mean value quantification where statistical data distribution is normal. Median quantification also showed robustness regardless of the observer's background by improving interobserver reproducibility of segmental native T1. The superiority of median T1 pixel value quantification compared with mean quantification is confirmed by better differentiation observed between patients with normal and abnormal heart function, especially in the septal regions that are least sensitive to susceptibility artifacts [31]. Therefore, median quantification would be a solution to reduce the influence of any unwanted outlier pixel-wise T1 values. Another study has already promoted MAD of fitting residuals to avoid outliers in the T1 fitting process yielding a robust measurement of native T1 [32].

In providing an early indication of cardiomyopathy disease in patients with normal cardiac MR functional parameters, native T1 showed no value according to several studies [11, 13, 15]. Our own results obtained with statistical parametric testing and (suboptimal) mean quantification also failed to differentiate between normal and abnormal heart function patients in LV segmental native T1 evaluation. In this study, however, significant increases of T1 values in abnormal heart function patients were found when using median T1 quantification with non-parametric testing instead. Our results also suggest that parametric testing must be performed

in native T1 quantification to make sure of statistical normality of the pixel-wise native T1 distribution prior to using means. Alternatively, one can simply use non-parametric testing and medians (as in this study) for the investigation of the patient heart condition.

Novel findings in this study of native T1 in normal heart function patients quantified by the medians in different myocardial coronary perfusion territories (i.e., LAD, right coronary artery, LCx, apical, mid-ventricular, and basal), different short-axis slices, and different AHA segments elaborate on those in smaller studies of healthy subjects [16, 19]. The observed variation of T1 value in the LV of normal heart function patients can provide regional baseline T1 values for early detection of diffuse fibrosis and infarct identification.

Suggested elsewhere [33–36], heart wall T1 elevation is related to coronary microvascular dysfunction (CMD). Camici et al [36] explained that morphological changes of CMD in the absence of myocardial diseases are characterized by microvascular remodeling, endothelial dysfunction, and smooth muscle dysfunction. In patients developing hypertrophic cardiomyopathy, remodeling of intramural coronary arterioles will result in medial and intimal wall thickening [36]. This study reported the elevation of native T1 values in different LV regions of abnormal functional heart patients. Moreover, the variation of native T1 value observed in normal patients between LAD and LCx coronary artery territories was absent in abnormal function heart patients, an observation that might indicate early progression of CMD. But to validate this relationship, more invasive and noninvasive clinical assessment is needed and therefore recommended for further study.

Limitations

Limitations of this study are that it is retrospective and that patient separation into those having a normal heart function and those without a normal heart function was based on the cardiac MR functional parameters defined by thresholds of just one reported study [25], being, however, very similar to those reported elsewhere [5, 8–12, 14, 15, 37–39]. The advice of some [17, 19, 40, 41], to correct native T1 for blood pool, heart rate, age, and gender were not followed through in this study due to the low correlation of T1 with any of these factors. Furthermore, the changes in native T1 values after correction were small and population-dependent (results not shown). Moreover, previous studies reported conflicting findings with regard to these factors' influence on native T1 value [10, 11, 18, 37, 42]. The T1 maps generated by custom-written software yielded slightly lower values with reduced deviations for all AHA segments compared with the values produced by

the Siemens Solution T1 maps (Supplementary Table S5). Investigations into T1 value differences amongst different mapping procedures and into alternative calculation algorithms to improve T1 fitting accuracy, for example [43], were not conducted, considered beyond the scope of this study.

Some studies reported the association between diabetes mellitus and the progression of CMD [36, 44, 45]. Another limitation of this study is that the diabetes mellitus status of the patients was not recorded.

Conclusion

In conclusion, T1 assessment by observations of medians showed higher interobserver reproducibility compared with mean T1, regardless of statistical normality of data. Increased robustness of myocardial native T1 assessed by pixel-wise medians thus facilitates the early detection of heart function impairment and differences between LV segments and between the different coronary artery territories.

Supplementary Chapter 5

Table S1 Characteristics of patients with normal and abnormal heart function according to the criteria of Kawel-Boehm et al. [25].

	Normal heart function (<i>n</i> = 26)	Abnormal heart function (<i>n</i> = 31)	<i>P</i> -Value ^a
General parameter			
Number of males	13 (50) ^b	17 (55) ^b	0.716 ^c
Age (years)	47 ± 19	41 ± 18	0.279 ^d
Heart rate (bpm)	67 ± 8	66 ± 7	0.706
BMI (kg/m ²)	25.15 ± 2.50	24.00 ± 2.60	0.481
BSA (m ²)	1.96 ± 0.22	1.97 ± 0.25	0.940 ^d
MR measured parameter			
Male			
LV mass (g)	113.32 ± 16.64	127.18 ± 36.23	0.174
LV mass index (g/m ²)	54.60 ± 8.02	61.08 ± 17.40	0.202
LV EDV (ml)	176.75 ± 20.13	220.85 ± 16.29	0.002
LV EDV index (ml/m ²)	85.16 ± 9.70	106.06 ± 7.82	0.002
LV ESV (ml)	71.69 ± 6.27	107.82 ± 14.79	< 0.001
LV ESV index (ml/m ²)	34.54 ± 3.02	51.78 ± 7.10	< 0.001
Stroke volume (ml)	101.52 ± 13.19	108.55 ± 11.73	0.517
LV EF (%)	59.52 ± 2.21	49.75 ± 2.52	< 0.001
Cardiac output (L/min)	7.70 ± 1.45	6.84 ± 0.94	0.621
Female			
LV mass (g)	72.24 ± 13.94	88.88 ± 17.61	0.012 ^d
LV mass index (g/m ²)	38.97 ± 7.52	48.51 ± 9.61	0.008 ^d
LV EDV (ml)	140.61 ± 18.04	183.50 ± 35.43	< 0.001 ^d
LV EDV index (ml/m ²)	75.85 ± 9.73	100.16 ± 19.34	0.001 ^d
LV ESV (ml)	53.00 ± 7.73	81.85 ± 10.27	< 0.001
LV ESV index (ml/m ²)	28.59 ± 4.17	44.67 ± 5.60	< 0.001
Stroke volume (ml)	87.42 ± 11.46	91.74 ± 19.58	0.495 ^d
LV EF (%)	62.23 ± 3.31	50.16 ± 6.91	< 0.001 ^d
Cardiac output (L/min)	5.66 ± 0.97	5.96 ± 1.89	0.615 ^d

Values are presented as mean ± standard deviation or median ± median absolute deviation. *n* number of patients, *bpm* beats per minute, *BMI* body mass index, *BSA* body surface area, *MR* magnetic resonance, *LV* left ventricle, *EDV* end diastolic volume, *ESV* end systolic volume, *EF* ejection fraction.

^a *P*-Values by Mann-Whitney U test.

^b Value is number of patients, with percentage in parentheses.

^c *P*-Value by chi square test.

^d *P*-Values by independent *t* test.

Table S2 T1 coefficient of variance between observers in different left ventricular myocardial regions.

	Patients with normal heart function						Patients with abnormal heart function					
	CoV between			CoV between			two cardiac			two non-cardiac		
	two cardiac experts using		two non-cardiac experts using	two cardiac experts using		two non-cardiac experts using	two cardiac experts using		two non-cardiac experts using	two cardiac experts using		two non-cardiac experts using
	Mean	Median	Mean	Median	Mean	Median	Mean	Median	Mean	Median	Mean	Median
Global LV myocardium	ns ^a	T1	5.73	4.95	4.90	4.44	ns ^a	T1	4.49	3.65	4.21	3.71
LAD	156	5.46	4.41	4.56	4.27	186	4.68	3.72	4.23	3.53	3.53	
RCA	130	5.41	4.76	3.04	2.78	155	4.08	3.27	3.33	2.91	2.91	
LCx	130	5.96	5.52	6.50	5.75	155	4.16	3.64	4.90	4.54	4.54	
Basal	156	4.09	3.05	3.40	2.83	186	3.34	2.59	3.63	2.87	2.87	
1 Anterior	26	5.10	2.90	3.14	2.48	31	4.71	3.61	5.67	3.80	3.80	
2 Anteroseptal	26	2.42	2.68	2.42	1.67	31	2.18	1.69	2.57	2.03	2.03	
3 Inferoseptal	26	3.04	2.64	2.09	2.41	31	2.00	1.14	2.43	2.47	2.47	
4 Inferior	26	2.68	1.78	2.58	1.75	31	3.25	2.86	3.17	2.94	2.94	
5 Inferolateral	26	1.63	1.25	3.31	2.34	31	2.34	1.83	3.41	2.53	2.53	
6 Anterolateral	26	5.71	4.64	5.53	4.95	31	3.70	2.81	3.28	2.81	2.81	
Mid-ventricular	156	4.92	3.83	5.29	5.03	186	4.30	3.08	4.08	3.65	3.65	
7 Anterior	26	4.95	4.14	6.42	6.82	31	6.19	4.64	4.87	4.59	4.59	
8 Anteroseptal	26	3.76	2.37	3.97	3.53	31	2.53	1.61	4.05	3.31	3.31	
9 Inferoseptal	26	1.64	1.38	1.52	1.15	31	2.11	1.31	2.19	1.42	1.42	
10 Inferior	26	4.63	2.37	2.72	2.66	31	3.64	2.88	2.51	2.64	2.64	
11 Inferolateral	26	3.07	2.66	6.05	5.75	31	2.94	2.35	3.90	3.05	3.05	
12 Anterolateral	26	6.34	6.34	7.74	7.02	31	4.70	3.06	5.85	5.57	5.57	

Apical	104	8.21	7.76	5.78	5.20	124	6.04	5.40	5.12	4.78
13 Anterior	26	8.24	8.01	5.75	5.67	31	6.10	5.67	4.97	4.28
14 Septal	26	2.69	2.20	3.27	2.47	31	3.26	2.61	2.01	2.27
15 Inferior	26	9.57	9.07	4.10	4.05	31	6.77	5.57	5.26	4.32
16 Lateral	26	8.93	8.67	8.47	7.40	31	5.64	6.05	6.87	6.95

Data are in percentage. *AHA* American Heart Association, *ns* number of segments, *CoV* coefficient of variance.

^a The number of segments reflects six combinations of segment comparisons between two observers.

Table S3 Shapiro-Wilk normality testing of native T1 segments in different left ventricular myocardial regions using mean quantification of pixel-wise values.

	ns ^a	Patients with normal heart function	ns ^a	Patients with abnormal heart function
		P-Value ^b of native T1		P-Value ^b of native T1
Global LV myocardium	2496	< 0.001	2976	< 0.001
LAD	936	< 0.001	1116	< 0.001
RCA	780	< 0.001	930	< 0.001
LCx	780	< 0.001	930	< 0.001
Basal	936	< 0.001	1116	< 0.001
1 Anterior	156	> 0.05	186	< 0.001
2 Anteroseptal	156	< 0.001	186	< 0.001
3 Inferoseptal	156	< 0.001	186	< 0.001
4 Inferior	156	< 0.01	186	< 0.001
5 Inferolateral	156	< 0.05	186	< 0.001
6 Anterolateral	156	< 0.001	186	< 0.001
Mid-ventricular	936	< 0.001	1116	< 0.001
7 Anterior	156	> 0.05	186	< 0.001
8 Anteroseptal	156	< 0.01	186	< 0.001
9 Inferoseptal	156	< 0.001	186	< 0.001
10 Inferior	156	< 0.001	186	< 0.001
11 Inferolateral	156	< 0.01	186	< 0.001
12 Anterolateral	156	< 0.001	186	< 0.001
Apical	624	< 0.001	744	< 0.001
13 Anterior	156	< 0.001	186	< 0.001
14 Septal	156	< 0.01	186	< 0.001
15 Inferior	156	< 0.001	186	0.056
16 Lateral	156	< 0.001	186	< 0.001

^a The number of segments reflects six combinations of segment comparisons between four observers.

^b P-Value of < 0.05 is considered as statistically significantly different from normal distribution.

Table S4 Shapiro-Wilk normality testing of native T1 segments in different left ventricular myocardial regions with using median quantification of pixel-wise values.

	ns ^a	Patients with normal heart function		Patients with abnormal heart function	
		<i>P</i> -Value ^b of native T1	ns ^a	<i>P</i> -Value ^b of native T1	
Global LV myocardium	2496	< 0.001	2976	< 0.001	
LAD	936	< 0.001	1116	< 0.001	
RCA	780	< 0.001	930	< 0.001	
LCx	780	< 0.001	930	< 0.001	
Basal	936	< 0.001	1116	< 0.001	
1 Anterior	156	< 0.01	186	< 0.001	
2 Anteroseptal	156	< 0.001	186	< 0.001	
3 Inferoseptal	156	< 0.001	186	< 0.001	
4 Inferior	156	< 0.001	186	< 0.001	
5 Inferolateral	156	< 0.01	186	< 0.001	
6 Anterolateral	156	< 0.001	186	< 0.001	
Mid-ventricular	936	< 0.001	1116	< 0.001	
7 Anterior	156	0.01	186	< 0.001	
8 Anteroseptal	156	> 0.05	186	< 0.001	
9 Inferoseptal	156	< 0.001	186	< 0.001	
10 Inferior	156	< 0.001	186	< 0.001	
11 Inferolateral	156	< 0.01	186	< 0.001	
12 Anterolateral	156	< 0.001	186	< 0.001	
Apical	624	< 0.001	744	< 0.001	
13 Anterior	156	< 0.001	186	< 0.001	
14 Septal	156	0.01	186	< 0.001	
15 Inferior	156	< 0.001	186	< 0.001	
16 Lateral	156	< 0.001	186	< 0.001	

^a The number of segments reflects six combinations of segment comparisons between four observers.

^b *P*-Value of < 0.05 is considered as statistically significantly different from normal distribution.

Table S5 Native T1 segments on different left ventricular myocardial regions of all patients using mean quantification of pixel-wise values.

		n	T1 value of all patients	T1 value of all	P-Value ^a
			evaluated by QMASS	patients evaluated by	
			Mean ± SD (ms)	MATLAB	
			Mean ± SD (ms)	Mean ± SD (ms)	
Basal					
1	Anterior	57	1017.00 ± 37.45 ^b	980.35 ± 36.49 ^b	0.001 ^c
2	Anteroseptal	57	1028.33 ± 58.81	990.69 ± 55.12	0.001
3	Inferoseptal	57	1027.57 ± 57.91	989.47 ± 54.29	< 0.001
4	Inferior	57	1032.91 ± 58.07	990.50 ± 55.27	< 0.001
5	Inferolateral	57	1006.09 ± 58.41	966.21 ± 53.68	< 0.001
6	Anterolateral	57	999.04 ± 52.72	962.32 ± 49.58	< 0.001
Mid-ventricular					
7	Anterior	57	1002.31 ± 41.29 ^b	965.37 ± 40.59 ^b	< 0.01 ^c
8	Anteroseptal	57	1004.93 ± 41.73 ^b	969.38 ± 40.12 ^b	0.001 ^c
9	Inferoseptal	57	1019.10 ± 57.72	982.28 ± 54.35	0.001
10	Inferior	57	1023.45 ± 40.00 ^b	987.55 ± 36.29 ^b	0.001 ^c
11	Inferolateral	57	997.31 ± 57.63	963.86 ± 56.02	< 0.01
12	Anterolateral	57	987.60 ± 66.65	952.63 ± 62.74	< 0.01
Apical					
13	Anterior	57	990.68 ± 87.32	954.51 ± 83.38	< 0.05
14	Septal	57	1018.12 ± 75.02	980.62 ± 70.06	< 0.01
15	Inferior	57	969.88 ± 111.76	935.01 ± 100.70	> 0.05
16	Lateral	57	981.72 ± 103.28	945.80 ± 98.62	> 0.05

SD, standard deviation; n, number of patients.

^a P-Values of T1 comparison evaluated by QMASS and MATLAB groups were made using independent sample *t* test.

^b Values are presented as median ± median absolute deviation.

^c P-Values of T1 comparison evaluated by QMASS and MATLAB groups were made using independent Mann-Whitney U test.

References

1. Puntmann VO, Peker E, Chandrashekar Y, Nagel E (2016) T1 Mapping in Characterizing Myocardial Disease. *Circulation Research* 119:277–299. <https://doi.org/10.1161/CIRCRESAHA.116.307974>
2. Raman FS, Kawel-Boehm N, Gai N, et al (2013) Modified look-locker inversion recovery T1 mapping indices: assessment of accuracy and reproducibility between magnetic resonance scanners. *Journal of cardiovascular magnetic resonance : official journal of the Society for Cardiovascular Magnetic Resonance* 15:64. <https://doi.org/10.1186/1532-429X-15-64>
3. Roujol S, Weingärtner S, Foppa M, et al (2014) Accuracy, precision, and reproducibility of four T1 mapping sequences: a head-to-head comparison of MOLLI, ShMOLLI, SASHA, and SAPHIRE. *Radiology* 272:683–9. <https://doi.org/10.1148/radiol.14140296>
4. Weingärtner S, Meßner NM, Budjan J, et al (2016) Myocardial T1-mapping at 3T using saturation-recovery: reference values, precision and comparison with MOLLI. *Journal of Cardiovascular Magnetic Resonance* 18:84. <https://doi.org/10.1186/s12968-016-0302-x>
5. Teixeira T, Hafyane T, Stikov N, et al (2016) Comparison of different cardiovascular magnetic resonance sequences for native myocardial T1 mapping at 3T. *Journal of Cardiovascular Magnetic Resonance* 18:65. <https://doi.org/10.1186/s12968-016-0286-6>
6. Kellman P, Hansen MS (2014) T1-mapping in the heart: Accuracy and precision. *Journal of Cardiovascular Magnetic Resonance* 16:2. <https://doi.org/10.1186/1532-429X-16-2>
7. Olivieri LJ, Kellman P, McCarter RJ, et al (2016) Native T1 values identify myocardial changes and stratify disease severity in patients with Duchenne muscular dystrophy. *Journal of cardiovascular magnetic resonance* 18:72. <https://doi.org/10.1186/s12968-016-0292-8>
8. Rogers T, Dabir D, Mahmoud I, et al (2013) Standardization of T1 measurements with MOLLI in differentiation between health and disease - the ConSept study. *Journal of Cardiovascular Magnetic Resonance* 15:78. <https://doi.org/10.1186/1532-429X-15-78>
9. Mordi I, Carrick D, Bezerra H, Tzemos N (2016) T1 and T2 mapping for early diagnosis of dilated non-ischaemic cardiomyopathy in middle-aged patients and differentiation from normal physiological adaptation. *European Heart Journal - Cardiovascular Imaging* 17:797–803. <https://doi.org/10.1093/ehjci/jev216>
10. Soslow JH, Damon SM, Crum K, et al (2016) Increased myocardial native T1 and extracellular volume in patients with Duchenne muscular dystrophy. *Journal of Cardiovascular Magnetic Resonance* 18:5. <https://doi.org/10.1186/s12968-016-0224-7>

11. Dabir D, Child N, Kalra A, et al (2014) Reference values for healthy human myocardium using a T1 mapping methodology: results from the International T1 Multicenter cardiovascular magnetic resonance study. *Journal of Cardiovascular Magnetic Resonance* 16:69. <https://doi.org/10.1186/s12968-014-0069-x>
12. Pica S, Sado DM, Maestrini V, et al (2014) Reproducibility of native myocardial T1 mapping in the assessment of Fabry disease and its role in early detection of cardiac involvement by cardiovascular magnetic resonance. *Journal of Cardiovascular Magnetic Resonance* 16:99. <https://doi.org/10.1186/s12968-014-0099-4>
13. Goebel J, Seifert I, Nensa F, et al (2016) Can Native T1 Mapping Differentiate between Healthy and Diffuse Diseased Myocardium in Clinical Routine Cardiac MR Imaging? *PLOS ONE* 11:e0155591. <https://doi.org/10.1371/journal.pone.0155591>
14. Yu L, Sun J, Sun J, et al (2018) Early detection of myocardial involvement by T₁ mapping of cardiac MRI in idiopathic inflammatory myopathy. *Journal of Magnetic Resonance Imaging* 48:415–422. <https://doi.org/10.1002/jmri.25945>
15. Treibel TA, Zemrak F, Sado DM, et al (2015) Extracellular volume quantification in isolated hypertension - changes at the detectable limits? *Journal of Cardiovascular Magnetic Resonance* 17:74. <https://doi.org/10.1186/s12968-015-0176-3>
16. Piechnik SK, Ferreira VM, Dall'Armellina E, et al (2010) Shortened Modified Look-Locker Inversion recovery (ShMOLLI) for clinical myocardial T1-mapping at 1.5 and 3 T within a 9 heartbeat breathhold. *Journal of cardiovascular magnetic resonance : official journal of the Society for Cardiovascular Magnetic Resonance* 12:69. <https://doi.org/10.1186/1532-429X-12-69>
17. Messroghli DR, Plein S, Higgins DM, et al (2006) Human myocardium: single-breath-hold MR T1 mapping with high spatial resolution--reproducibility study. *Radiology* 238:1004–12. <https://doi.org/10.1148/radiol.2382041903>
18. Chin CWL, Semple S, Malley T, et al (2014) Optimization and comparison of myocardial T1 techniques at 3T in patients with aortic stenosis. *European Heart Journal - Cardiovascular Imaging* 15:556–565. <https://doi.org/10.1093/ehjci/jet245>
19. Reiter U, Reiter G, Dorr K, et al (2014) Normal diastolic and systolic myocardial T1 values at 1.5-T MR imaging: correlations and blood normalization. *Radiology* 271:365–72. <https://doi.org/10.1148/radiol.13131225>
20. Cameron D, Vassiliou VS, Higgins DM, Gatehouse PD (2018) Towards accurate and precise T₁ and extracellular volume mapping in the myocardium: a guide to current pitfalls and their solutions. *Magnetic Resonance Materials in Physics, Biology and Medicine* 31:143–163. <https://doi.org/10.1007/s10334-017-0631-2>
21. Saiviroonporn P, Viprakasit V, Boonyasirinant T, et al (2011) Comparison of the region-based and pixel-wise methods for cardiac T2* analysis in 50 transfusion-dependent Thai thalassemia patients. *Journal of computer assisted tomography* 35:375–81. <https://doi.org/10.1097/RCT.0b013e31820eaaf2>

22. Ferguson MR, Otto RK, Bender MA, et al (2013) Liver and heart MR relaxometry in iron loading: reproducibility of three methods. *Journal of magnetic resonance imaging: JMRI* 38:987–90. <https://doi.org/10.1002/jmri.23937>
23. Positano V, Meloni A, Santarelli MF, et al (2015) Fast generation of T2* maps in the entire range of clinical interest: application to thalassemia major patients. *Computers in biology and medicine* 56:200–10. <https://doi.org/10.1016/j.compbiomed.2014.10.020>
24. Roller FC, Kriechbaum S, Breithecker A, et al (2019) Correlation of native T1 mapping with right ventricular function and pulmonary haemodynamics in patients with chronic thromboembolic pulmonary hypertension before and after balloon pulmonary angioplasty. *European Radiology* 29:1565–1573. <https://doi.org/10.1007/s00330-018-5702-x>
25. Kawel-Boehm N, Maceira A, Valsangiacomo-Buechel ER, et al (2015) Normal values for cardiovascular magnetic resonance in adults and children. *Journal of cardiovascular magnetic resonance: official journal of the Society for Cardiovascular Magnetic Resonance* 17:29. <https://doi.org/10.1186/s12968-015-0111-7>
26. Xue H, Shah S, Greiser A, et al (2012) Motion correction for myocardial T1 mapping using image registration with synthetic image estimation. *Magnetic resonance in medicine* 67:1644–55. <https://doi.org/10.1002/mrm.23153>
27. Rinta-Kiikka I, Tuohinen S, Ryymin P, et al (2014) Correlation of Electrocardiogram and Regional Cardiac Magnetic Resonance Imaging Findings in ST-Elevation Myocardial Infarction: A Literature Review. *Annals of Noninvasive Electrocardiology* 19:509–523. <https://doi.org/10.1111/anec.12210>
28. Saïda A Ben (2014) Shapiro-Wilk and Shapiro-Francia normality tests. In: MATLAB Central File Exchange. <https://nl.mathworks.com/matlabcentral/fileexchange/13964-shapiro-wilk-and-shapiro-francia-normality-tests>. Accessed 24 Mar 2017
29. Leys C, Ley C, Klein O, et al (2013) Detecting outliers: Do not use standard deviation around the mean, use absolute deviation around the median. *Journal of Experimental Social Psychology* 49:764–766. <https://doi.org/10.1016/j.jesp.2013.03.013>
30. Rousseeuw PJ, Croux C (1993) Alternatives to the Median Absolute Deviation. *Journal of the American Statistical Association* 88:1273–1283. <https://doi.org/10.1080/01621459.1993.10476408>
31. Messroghli DR, Moon JC, Ferreira VM, et al (2017) Clinical recommendations for cardiovascular magnetic resonance mapping of T1, T2, T2* and extracellular volume: A consensus statement by the Society for Cardiovascular Magnetic Resonance (SCMR) endorsed by the European Association for Cardiovascular Imaging (EACVI). *Journal of Cardiovascular Magnetic Resonance* 19:75. <https://doi.org/10.1186/s12968-017-0389-8>

32. Kellman P, Arai AE, Xue H (2013) T1 and extracellular volume mapping in the heart: estimation of error maps and the influence of noise on precision. *Journal of cardiovascular magnetic resonance : official journal of the Society for Cardiovascular Magnetic Resonance* 15:56. <https://doi.org/10.1186/1532-429X-15-56>
33. Liu A, Wijesurendra RS, Francis JM, et al (2016) Adenosine Stress and Rest T1 Mapping Can Differentiate Between Ischemic, Infarcted, Remote, and Normal Myocardium Without the Need for Gadolinium Contrast Agents. *JACC: Cardiovascular Imaging* 9:27–36. <https://doi.org/10.1016/J.JCMG.2015.08.018>
34. Arnold JR, Karamitsos TD, Bhamra-Ariza P, et al (2012) Myocardial Oxygenation in Coronary Artery Disease: Insights From Blood Oxygen Level–Dependent Magnetic Resonance Imaging at 3 Tesla. *Journal of the American College of Cardiology* 59:1954–1964. <https://doi.org/10.1016/J.JACC.2012.01.055>
35. Ferreira VM (2018) T1 Mapping of the Remote Myocardium. *Journal of the American College of Cardiology* 71:779–781. <https://doi.org/10.1016/j.jacc.2017.12.021>
36. Camici PG, d’Amati G, Rimoldi O (2015) Coronary microvascular dysfunction: mechanisms and functional assessment. *Nature Reviews Cardiology* 12:48–62. <https://doi.org/10.1038/nrcardio.2014.160>
37. Liu CY, Liu YC, Wu C, et al (2013) Evaluation of age-related interstitial myocardial fibrosis with cardiac magnetic resonance contrast-enhanced T1 mapping: MESA (Multi-Ethnic Study of Atherosclerosis). *Journal of the American College of Cardiology* 62:1280–1287. <https://doi.org/10.1016/j.jacc.2013.05.078>
38. Fonarow GC, Hsu JJ (2016) Left Ventricular Ejection Fraction: What Is “Normal”? *JACC: Heart Failure* 4:511–513. <https://doi.org/10.1016/J.JCHF.2016.03.021>
39. Petersen SE, Aung N, Sanghvi MM, et al (2017) Reference ranges for cardiac structure and function using cardiovascular magnetic resonance (CMR) in Caucasians from the UK Biobank population cohort. *Journal of Cardiovascular Magnetic Resonance* 19:18. <https://doi.org/10.1186/s12968-017-0327-9>
40. Piechnik SK, Ferreira VM, Lewandowski AJ, et al (2013) Normal variation of magnetic resonance T1 relaxation times in the human population at 1.5 T using ShMOLLI. *Journal of cardiovascular magnetic resonance* 15:13. <https://doi.org/10.1186/1532-429X-15-13>
41. Nickander J, Lundin M, Abdula G, et al (2017) Blood correction reduces variability and gender differences in native myocardial T1 values at 1.5 T cardiovascular magnetic resonance – a derivation/validation approach. *Journal of Cardiovascular Magnetic Resonance* 19:41. <https://doi.org/10.1186/s12968-017-0353-7>
42. Rauhala SMO, Mangion K, Barrientos PH, et al (2016) Native myocardial longitudinal ($T_{1\rho}$) relaxation time: Regional, age, and sex associations in the healthy adult heart. *Journal of Magnetic Resonance Imaging* 44:541–548. <https://doi.org/10.1002/jmri.25217>

43. Shao J, Liu D, Sung K, et al (2017) Accuracy, precision, and reproducibility of myocardial T1 mapping: A comparison of four T1 estimation algorithms for modified look-locker inversion recovery (MOLLI). *Magnetic Resonance in Medicine* 78:1746–1756. <https://doi.org/10.1002/mrm.26565>
44. Crea F, Camici PG, Bairey Merz CN (2014) Coronary microvascular dysfunction: an update. *European Heart Journal* 35:1101–1111. <https://doi.org/10.1093/eurheartj/ehf513>
45. Dal Lin C, Tona F, Osto E (2015) Coronary Microvascular Function and Beyond: The Crosstalk between Hormones, Cytokines, and Neurotransmitters. *International Journal of Endocrinology* 2015:1–17. <https://doi.org/10.1155/2015/312848>

Myocardial perfusion

